Inorganic Chemistry

Article

pubs.acs.org/IC

Shedding Light on the Photochemistry of Coinage-Metal Phosphorescent Materials: A Time-Resolved Laue Diffraction Study of an Ag^{I}–Cu^{I} Tetranuclear Complex

Katarzyna N. Jarzembska,*[,†,‡] Radosław Kamiński,[†] Bertrand Fournier,[†] Elżbieta Trzop,[†] Jesse D. Sokolow,[†] Robert Henning,[§] Yang Chen,[†] and Philip Coppens*[,†]

[†]Department of Chemistry, University at Buffalo, The State University of New York, Buffalo, New York 14260-3000, United States

[‡]Department of Chemistry, University of Warsaw, Pasteura 1, 02-093 Warszawa, Poland

[§]Consortium for Advanced Radiation Sources, University of Chicago, Chicago, Illinois 60637, United States

Supporting Information

ABSTRACT: The triplet excited state of a new crystalline form of a tetranuclear coordination d^{10}–d^{10}-type complex, $Ag_2Cu_2L_4$ (L = 2-diphenylphosphino-3-methylindole ligand), containing Ag^{I} and Cu^{I} metal centers has been explored using the Laue pump–probe technique with ≈80 ps time resolution. The relatively short lifetime of 1 μs is accompanied by significant photoinduced structural changes, as large as the Ag1···Cu2 distance shortening by 0.59(3) Å. The results show a pronounced strengthening of the argentophilic interactions and formation of new Ag···Cu bonds on excitation. Theoretical calculations indicate that the structural changes are due to a ligand-to-metal charge transfer (LMCT) strengthening the Ag···Ag interaction, mainly occurring from the methylindole ligands to the silver metal centers. QM/MM optimizations of the ground and excited states of the complex support the experimental results. Comparison with isolated molecule optimizations demonstrates the restricting effect of the crystalline matrix on photoinduced distortions. The work represents the first time-resolved Laue diffraction study of a heteronuclear coordination complex and provides new information on the nature of photoresponse of coinage metal complexes, which have been the subject of extensive studies.

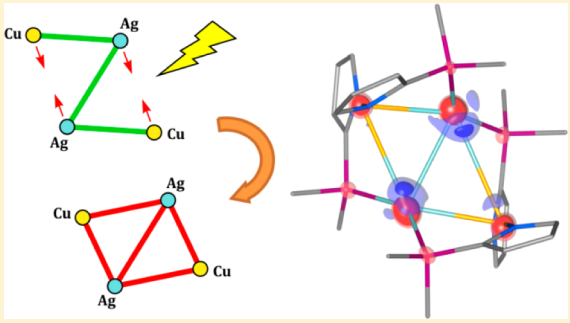

1. INTRODUCTION

Coordination complexes of coinage metals have attracted considerable attention thanks to their rich electronic and luminescent properties, which are of importance in the design of molecular devices and functional materials.[1−7] Among this class of compounds, polynuclear d^{10} complexes exhibit a considerable structural diversity. Their photochemical properties can be modified by the choice of ligands and/or by variation of the number of metal centers, thereby allowing fine-tuning of the HOMO–LUMO energy levels and the resulting luminescence.[8−14] Various d^{10} gold complexes show short metal···metal contacts. Schmidbaur introduced the term aurophilicity[15] for the Au···Au interactions, which involve important electron correlation/dispersion forces and relativistic effects, analyzed in detail by Pyykkö in a series of articles.[16−18] Somewhat weaker, but still important, argentophilic and cuprophilic interactions have been recognized in numerous studies.[5,9−17,19−41] A number of examples of short argentophilic contacts down to 2.637(1) Å, found in $[Et_4N]_2[(Ag(Sn_2B_{11}H_{11})bipy)_2]$,[41] have been reported.[19,21,42−44] In particular, heterometallic complexes[9,12,27,29,32,45−49] have recently attracted interest because of their efficient luminescence.

The short metallophilic contacts encountered in these complexes considerably affect the nature of the lowest lying emissive states.[9,12,26,39] Thus, information on structural changes and charge transfer (CT) occurring on excitation is relevant for rational design of new materials. Such information is now becoming available. Time-resolved X-ray absorption techniques have been employed to obtain local information, in particular on changes in the coordination of the fluorescing atoms. Among the complexes studied are those of Ru^{II}, Ni^{II}, and Fe^{II}.[50−55]

More detailed analysis of excited-state structures of short-lived species in the solid state is possible by exploitation of synchrotron sources combined with advanced experimental methods.[56] Recent advances in application of the pink-Laue time-resolved (TR) synchrotron technique,[57−60] using modified data collection[61] and data processing procedures,[62−64] have speeded the application of the method, which is, by its nature, limited by the ≈100 ps temporal resolution of synchrotron sources. However, this resolution suffices for the study of phosphorescence and many fluorescence processes. Several such studies have now been reported.[57,65−68]

We here report the first synchrotron TR diffraction study of a polynuclear d^{10}–d^{10} coordination compound ($Ag_2Cu_2L_4$, L = 2-

Received: July 16, 2014
Published: September 19, 2014

   dx.doi.org/10.1021/ic501696y | Inorg. Chem. 2014, 53, 10594−10601

diphenylphosphino-3-methylindole ligand; **1**) (Figure 1). Results are compared with those of parallel theoretical calculations using time-dependent DFT (TDDFT) and the quantum-mechanics/molecular-mechanics (QM/MM) methods.

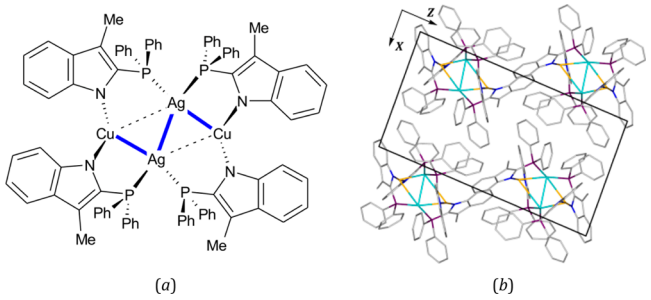

Figure 1. (a) Ground-state molecular structure of the $Ag_2Cu_2L_4$ complex (**1**) (Ag···Ag and two shorter Ag···Cu interactions are shown in bold). (b) Packing diagram of the new solvent-free crystal form of **1**.

2. EXPERIMENTAL SECTION

2.1. Crystal Synthesis and Ground-State Structure Determination. Synthesis of the $Ag_2Cu_2L_4$ complex was carried out according to a literature procedure.[47] A solvent-free crystal form was obtained by replacing chloroform ($CHCl_3$) with methylene dichloride (CH_2Cl_2) during the crystallization process. Its crystal structure was determined using standard single-crystal X-ray methods at 90 K. Details on the X-ray diffraction data collection and processing are described in the Supporting Information. Similar to that for the previously reported structure, the new crystal form belongs to the $P\bar{1}$ space group with one molecule in the asymmetric part of the unit cell.[69] Crystal packing is shown in Figure 1b. Geometric features of **1** are very similar in both solid forms.

2.2. Spectroscopy. A solution of complex **1** in methylene dichloride is reported to show absorption maxima at 290 and 450 nm.[47] A broad absorption band in a wavelength range extending up to 550 nm occurs in the solid-state spectrum (Figure S1a, Supporting Information). Both chloroform-solvated and solvent-free crystals are red luminescent materials with room temperature emission maxima at 650 nm upon excitation with ≈350−400 nm light (Figure S1b, Supporting Information). The emission maximum also occurs at the same wavelength at 90 K, at which the decay is biexponential (Figure S1c, Supporting Information) with lifetimes of 0.16(1) and 0.98(1) μs. The large Stokes shift is typical for a significant structural rearrangement, while the close to microsecond lifetime of the second emission indicates a triplet excited state. Further details are presented in Section 1.1 of the Supporting Information.

2.3. Time-Resolved X-ray Diffraction. Laue data sets were collected at a 15 keV undulator setting, which corresponds to a λ range of ≈0.8−1.1 Å.[57] Small crystals, of ≈20 × 30 × 70 μm^3 average size, were used in order to minimize inhomogeneous exposure of the sample due to lack of penetration of the laser beam. The sample was excited with 38 ps, 390 nm laser pulses from a Ti:sapphire laser with a power of 0.25−0.50 mJ·mm^{-2} per pulse. It was subsequently probed by the ≈80 ps wide X-ray pulse with a pump−probe delay of 100 ps. For each set of angles, alternate ON and OFF frames were collected repeatedly to improve the statistics of the experimental intensity ratios[61] (I^{ON}/I^{OFF}), as described in Kalinowski et al.[62] Four good quality data sets were collected and processed with the *LAUEUTIL* toolkit.[62,63]

2.4. Refinement of the Laser-Induced Response. Refinements with the program *LASER*[70] are based on the intensity ratios (I^{ON}/I^{OFF}) with separate population and temperature scale factors for each of the data sets (Supporting Information). The random excited-state distribution model[71] was used in the refinement. Positions of the strongly scattering metal atoms were freely refined, whereas the eight ligand fragments, i.e., four methylindoles and four phenylphosphines, were treated as rigid bodies anchored on the respective nitrogen and phosphorus atoms. The ground-state geometry from the monochromatic data was restricted as a rigid body in the *LASER* refinement. Data refinement strategy of the structural changes based on the response ratios consisted of several steps in which the Ag and Cu atom positions, population factors, ligand positions, ligand orientations, and temperature scale factors were refined alternately in blocks. In the final step, all excited-state parameters were refined together with the ground-state rigid body translational and rotational parameters. Full details can be found in Section 1.4 of the Supporting Information.

2.5. Theoretical Calculations. In order to understand the nature of the excitation and the effect of the confining crystal environment,

Table 1. Bond Distances, Valence Angles, and Atomic Shifts for the Light-OFF (GS) and Light-ON (ES) Structures Together with the Computed Parameter Changes upon Light Exposure[a]

	experiment			theory (QM/MM)			theory (isolated molecule)		
bond	$d^{GS}_{X\cdots Y}$/Å	$d^{ES}_{XE\cdots YE}$/Å	Δd/Å	$d^{GS}_{X\cdots Y}$/Å	$d^{ES}_{XE\cdots YE}$/Å	Δd/Å	$d^{GS}_{X\cdots Y}$/Å	$d^{ES}_{XE\cdots YE}$/Å	Δd/Å
Ag1···Ag2	3.0345(2)	2.66(3)	−0.38(3)	3.094	2.749	−0.345	3.329	2.795	−0.534
Ag1···Cu1	2.7640(2)	2.82(3)	+0.06(3)	2.746	2.832	+0.086	2.732	2.952	+0.220
Ag1···Cu2	3.4655(2)	2.88(3)	−0.59(3)	3.736	3.114	−0.622	3.891	2.960	−0.931
Ag2···Cu1	3.2110(2)	2.93(3)	−0.29(3)	3.462	3.024	−0.438	3.891	2.959	−0.932
Ag2···Cu2	2.8043(2)	2.70(3)	−0.10(3)	2.775	2.822	+0.047	2.732	2.953	+0.221
angle	$\theta^{GS}_{X\cdots Y\cdots Z}$/deg	$\theta^{ES}_{X\cdots Y\cdots Z}$/deg	$\Delta\theta$/deg	$\theta^{GS}_{X\cdots Y\cdots Z}$/deg	$\theta^{ES}_{X\cdots Y\cdots Z}$/deg	$\Delta\theta$/deg	$\theta^{GS}_{X\cdots Y\cdots Z}$/deg	$\theta^{ES}_{X\cdots Y\cdots Z}$/deg	$\Delta\theta$/deg
Ag1···Cu1···Ag2	60.495(4)	54.33(1)	−6.16(1)	58.45	55.89	−2.56	57.18	56.43	−0.75
Cu1···Ag2···Cu2	124.072(7)	125.80(1)	+1.72(1)	125.88	126.05	+0.17	119.55	123.57	+4.02
Ag2···Cu2···Ag1	56.720(4)	56.09(1)	−0.63(1)	54.37	54.91	+0.54	57.19	56.41	−0.78
Cu2···Ag1···Cu1	116.724(7)	123.09(1)	+6.36(1)	117.43	122.35	+4.92	119.57	123.59	+4.02
atomic shifts	$d_{X\cdots XE}$/Å			$d_{X\cdots XE}$/Å					
Ag1 → Ag1E	0.30(2)			0.43					
Ag2 → Ag2E	0.27(1)			0.39					
Cu1 → Cu1E	0.09(2)			0.10					
Cu2 → Cu2E	0.33(2)			0.26					

[a]GS atoms are labeled as in the original structure; ES atoms are denoted with the letter E. Parameter changes are the differences between ES and GS geometries. The experimental values are compared with the analogous results obtained with the QM/MM approach and with isolated-molecule optimizations.

dx.doi.org/10.1021/ic501696y | *Inorg. Chem.* 2014, 53, 10594−10601

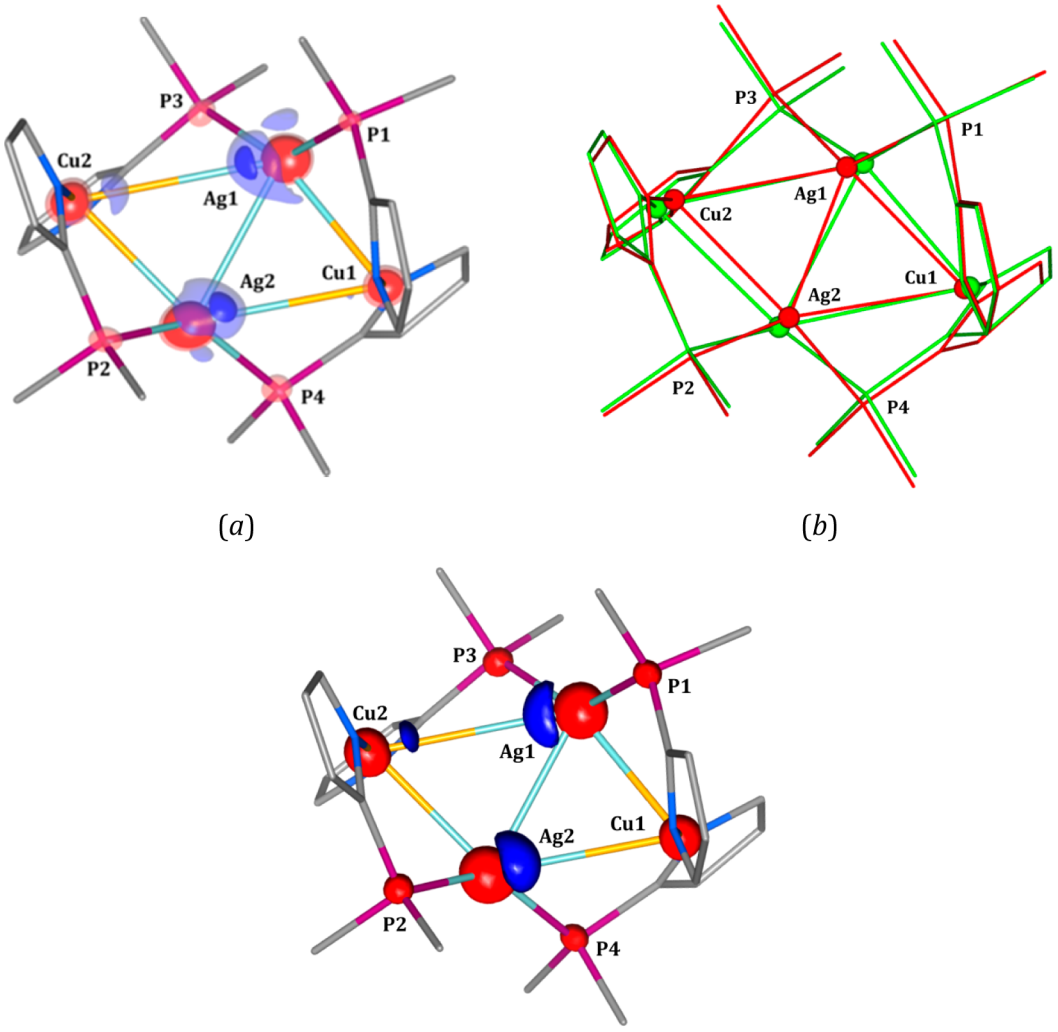

Figure 2. (a) Photodifference map ($F_o^{ON} - F_o^{OFF}$) of complex **1** showing atomic shifts upon excitation (solid isosurfaces, ±0.55 e·Å^{-3}; semitransparent, ±0.35 e·Å^{-3}; blue, positive; red, negative). (b) Refined excited-state geometry related to that of the ground-state crystal structure (green, ground state; red, excited state; methylindole ligands were omitted for clarity). (c) Photodeformation map ($F_c^{ON} - F_c^{OFF}$) of **1** based on the refined model parameters (isosurfaces, ± 0.30 e·Å^{-3}; blue, positive; red, negative; k_B = 1.06).

three types of calculations were performed. They include time-dependent DFT (TDDFT) computations of the spectroscopic transitions[72,73] using the GS experimental geometry, with the C−H bond distances fixed at neutron-normalized values,[74,75] and isolated molecule and QM/MM[76−79] optimizations of both the GS and ES to account for the effect of the surrounding crystal lattice. The PBE0 functional[80,81] and LANL2DZ basis set[82−85] were used in the analyses with the *GAUSSIAN* package.[86] Results are listed in Table 1. The Hirshfeld[87] and Bader atom charges and topological properties[88] were calculated with the *ADF* package[89−93] at the DFT(BP86)/TZP level of theory[94−98] with the zero-order regular approximation (ZORA).[99−103] Further details on the calculations are given in Section 1.5 of the Supporting Information.

3. RESULTS AND DISCUSSION

3.1. Photodifference Maps. Photodifference maps[57,104−106] are a prime tool for deriving an initial starting structure for subsequent least-squares refinement. As shown in Figure 2a, pronounced peaks occur in the vicinity of the silver atoms and the Cu2 copper atom, whereas the features near Cu1 are much weaker. The location of the positive peaks is a sign that the bonds between the Ag and Cu atoms shorten on excitation, leading to a rhomb-shaped rather than the Z-shaped arrangement of the metal atoms observed in the ground state. This conclusion is confirmed by the subsequent least-squares refinement with the program *LASER*.[70]

Table 2. TDDFT-Calculated Main Orbital Contributions to the LMCT Singlet−Singlet Transitions[a]

main orbital contributions	E/eV	λ/nm	$f\cdot10^4$
HOMO → LUMO	2.6721	463.99	154
HOMO-1 → LUMO	2.7340	453.49	281
HOMO-2 → LUMO	2.8689	432.17	143
HOMO-3 → LUMO	2.9573	419.25	34

[a] E, energy; f, oscillator strength.

3.2. Refinement Results. In the structural refinement performed with the program *LASER*, the temperature changes of the crystals upon irradiation are accounted for by a temperature scale factor k_B multiplying all GS thermal parameters ($U_{ij}^{ON} = k_B \cdot U_{ij}^{OFF}$). k_B ranged from 1.035 to 1.064 in the four data sets collected (Table S5, Supporting Information), which, in the classical harmonic limit, corre-

dx.doi.org/10.1021/ic501696y | *Inorg. Chem.* 2014, 53, 10594−10601

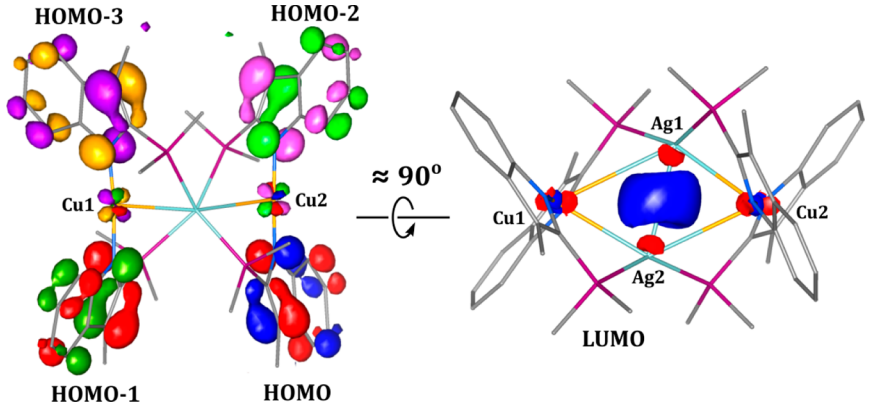

Figure 3. Composite picture of the molecular orbitals with the most significant contribution to the LMCT transition (PBE0/LANL2DZ). ±0.06 au contours; left panel, view along Ag2 → Ag1 direction showing a composite of the four highest occupied MOs; right panel, top view. Phenyl rings are omitted for clarity.

Table 3. Decomposition of Selected Molecular Orbitals into Atomic and Ligand Percentage Contributions[a]

orbital	HOMO	HOMO-1	HOMO-2	HOMO-3	LUMO
energy, *E*/eV	−5.05	−5.13	−5.23	−5.34	−1.64
Ag1	0%	0%	0%	0%	24%
Ag2	0%	0%	0%	0%	23%
Cu1	0%	5%	0%	4%	7%
Cu2	5%	0%	4%	0%	6%
N1 indole	70%	3%	19%	1%	1%
N2 indole	1%	67%	4%	22%	1%
N3 indole	20%	0%	68%	6%	1%
N4 indole	0%	23%	4%	64%	1%
P1 ligand	0%	1%	0%	0%	10%
P2 ligand	1%	0%	0%	0%	7%
P3 ligand	0%	0%	0%	0%	10%
P4 ligand	0%	0%	0%	0%	9%

[a]PBE0/LANL2DZ level of theory.

sponds to a 3−6 K temperature increase, in good agreement with the slope of the photo-Wilson plot[107] obtained prior to the refinement. The refined population of the excited-state species ranged from 0.5 to 1.7% in the four data sets (Table S5, Supporting Information). The small conversion percentage is a result of the need to keep the laser power down to prevent frequent loss of the sample crystals, but it is also a result of the moderate quantum yield of emission reported previously.[47] The most relevant geometrical parameters are summarized in Table 1. Additional refinement details are listed in the Supporting Information.

As anticipated from the large Stokes shift, the observed changes on excitation are considerable, reaching 0.59(3) and 0.38(3) Å for the Ag1···Cu2 and Ag1···Ag2 distances, respectively. The changes in position of the lightly scattering P and N atoms are less significant given the large standard deviations estimated both for the atomic shifts (especially of N atoms) and for the rigid-body rotations (Supporting Information).

A considerable contraction on excitation from 3.0345(2) to 2.66(3) Å is observed for the Ag···Ag distance. The resulting excited bond length is far below the sum of the corresponding van der Waals radii (3.44 Å),[108] but it is comparable to those of some strong argentophilic ground-state contacts reported, such as 2.637(1) Å found in $[Et_4N]_2[(Ag(Sn_2B_{11}H_{11})bipy)_2]$[41] and 2.725(1) Å in $[(\mu\text{-NHC})_3Ag_3](BF_4)_3$.[19] In turn, the GS value is characteristic for weakly interacting silver centers.[21,36,109]

The large contraction of the long Ag1···Cu2 and Ag2···Cu1 distances and the slight elongation of the short Ag1···Cu1 have the effect almost equalizing all Ag···Cu contacts at values shorter than the sum of the corresponding van der Waals radii. Collectively, this results in a dramatic change of the Z-shaped GS geometry of the complex in the crystal to a rhomb-shaped pattern of the metal atoms in the excited state (Figure 2b). The photodeformation map (Figure 2c), calculated with the refined model parameters, shows the significant atomic shifts. The large geometrical changes upon excitation provide an explanation for the easy breakdown of the crystals in the laser beam noticed earlier.

3.3. Theoretical Analysis. The TDDFT calculations, performed both at the BP86/TZP level of theory with ZORA

Table 4. Electron Density (ϱ) and Laplacian ($\nabla^2\varrho$) Values at BCPs Calculated for the Experimental and QM/MM-Optimized GS and ES Geometries[a]

	experimental geometry				QM/MM geometry			
	GS		ES		GS		ES	
bond	$\varrho(r_{BCP})$/e·Å^{-3}	$\nabla^2\varrho(r_{BCP})$/e·Å^{-5}	$\varrho(r_{BCP})$/e·Å^{-3}	$\nabla^2\varrho(r_{BCP})$/e·Å^{-5}	$\varrho(r_{BCP})$/e·Å^{-3}	$\nabla^2\varrho(r_{BCP})$/e·Å^{-5}	$\varrho(r_{BCP})$/e·Å^{-3}	$\nabla^2\varrho(r_{BCP})$/e·Å^{-5}
Ag1···Ag2	0.147	1.292	0.322	2.793	0.131	1.129	0.270	2.215
Ag1···Cu1	0.204	1.585	0.193	1.351	0.207	1.655	0.184	1.333
Ag1···Cu2	[b]	[b]	0.184	1.170	[b]	[b]	0.130	0.670
Ag2···Cu1	0.105[c]	0.661[c]	0.166	1.065	[b]	[b]	0.143	0.842
Ag2···Cu2	0.191	1.441	0.233	1.861	0.198	1.519	0.187	1.360

[a]DFT(BP86)/TZP/ZORA level of theory. [b]No BCP found. [c]The electron density and Laplacian values are significantly smaller (ca. factor of 2) than that for other Ag···Cu interactions.

dx.doi.org/10.1021/ic501696y | Inorg. Chem. 2014, 53, 10594−10601

Table 5. Hirshfeld (Q_H) and QTAIM Bader (Q_B) Atomic and Ligand Charges Computed at the Experimental Geometries of the Ground State (GS) and Excited States (ES) at the DFT(BP86)/TZP/ZORA Level of Theory[a]

atom/ligand	Q_H^{GS}/e	Q_H^{ES}/e	ΔQ_H/e	Q_B^{GS}/e	Q_B^{ES}/e	ΔQ_B/e
Ag1	+0.144	+0.063	−0.081	+0.165	+0.034	−0.131
Ag2	+0.130	+0.059	−0.071	+0.125	+0.008	−0.117
Cu1	+0.209	+0.203	−0.006	+0.538	+0.555	+0.018
Cu2	+0.212	+0.205	−0.007	+0.539	+0.556	+0.017
P1 ligand	+0.193	+0.146	−0.047	+0.639	+0.425	−0.214
P2 ligand	+0.186	+0.164	−0.022	+0.644	+0.578	−0.066
P3 ligand	+0.196	+0.160	−0.036	+0.652	+0.556	−0.096
P4 ligand	+0.211	+0.131	−0.081	+0.663	+0.506	−0.157
N1 indole	−0.351	−0.276	+0.075	−1.001	−0.742	+0.260
N2 indole	−0.374	−0.268	+0.106	−0.989	−0.796	+0.193
N3 indole	−0.382	−0.297	+0.085	−0.988	−0.850	+0.138
N4 indole	−0.373	−0.289	+0.085	−0.984	−0.830	+0.154

[a]Charge changes (ΔQ) are the differences between ES and GS.

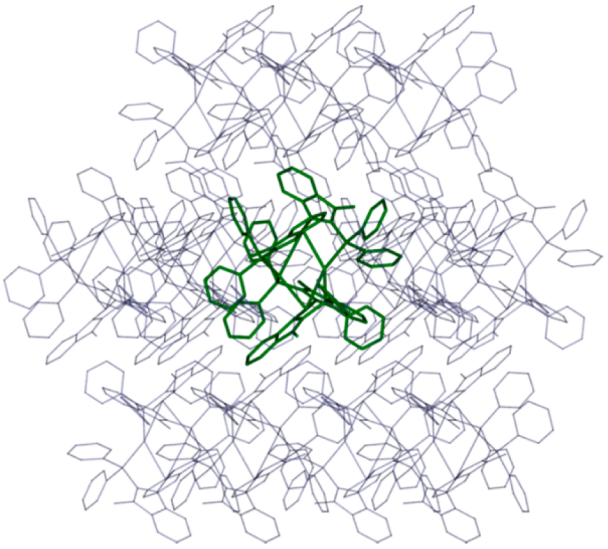

Figure 4. Molecule shell used in the QM/MM calculations (green, central molecule; gray, shell of 13 molecules within a radius of 10 Å). The input files were prepared with the aid of the *CLUSTERGEN* program.[78]

and PBE0/LANL2DZ, show that the main transitions involve excitations from each of the four of the highest occupied molecular orbitals (HOMO, HOMO-1, HOMO-2, and HOMO-3; Table 2 and Supporting Information), which are mainly located on each of the four indole ligands, as illustrated in Figure 3. These orbitals consists generally of the p atomic orbitals of the indole carbon and nitrogen atoms, as shown in Tables 3 and S11, with some minor d_{xy} contributions from the Cu atoms (coordinate system: Z along the Ag1 → Ag2 direction, X axis perpendicular, and Y axis parallel to the metal atom's mean plane, as illustrated in Figure S5).

The cluster-centered lowest unoccupied molecular orbital (LUMO) is the acceptor in the four lowest energy transitions, which have the largest oscillator strengths in the visible region (Table 2). The LUMO is centered on the Ag_2Cu_2 core and involves the 5s and $5p_z$ atomic Ag orbitals, with relative contributions of 8 and 13% on each Ag atom, respectively, directed along the Ag−Ag axis (Figure 3, Table S11). The resulting transition, which corresponds to a ligand-to-metal charge transfer (LMCT) strengthening the Ag···Ag interaction, is similar to that reported for an Au_2Ag_2 cluster by Laguna et al.[9] The estimated contribution of the silver atomic orbitals to the LUMO reaches about 50%, while the remaining percentage is accounted for mostly by the $3d_{x^2-y^2}$ orbitals of the Cu atoms and p orbitals of the phosphine ligands (Tables 3 and S11). The results indicate pσ-bond formation between the two silver centers. The d orbitals on the silver atom do not contribute to the transition, as reported for other cases.[31,34,37] σ bond formation upon excitation was also suggested for other complexes of the kind.[39,40]

Quantum theory of atoms in molecules (QTAIM) analysis of the charge density in both the GS and ES, based on the experimentally determined geometries, shows an increase in the positive Laplacian at the Ag···Ag bond critical point (BCP) between the GS and ES from 1.29 to 2.79 e·Å^{-5}. The electron density at this BCP rises from 0.15 to 0.32 e·Å^{-3}. The latter value is comparable with those reported in the literature for stable metal···metal bonds.[110−112] A corresponding increase is calculated for the Ag1···Cu2 and Ag2···Cu1 interactions (Table 4). According to the topological analysis, both the GS Ag1···Cu2 and Ag2···Cu1 contacts become weak intermetallic bonds. All of the Ag···Ag and Ag···Cu interactions can be classified as being of the closed-shell type.

Net charges in the GS and ES are summarized in Table 5. As mentioned above, the observed low-energy charge transfer can be described as a LMCT, i.e., $\pi \rightarrow \sigma$, what is typical for this class of compounds.[34] The indole fragments are the charge donors, whereas the silver atoms and, to much a lesser degree, phosphine groups bonded to Ag are the CT acceptors. The two copper atoms are also affected by the charge transfer as their d-orbital populations change, although their atomic charges remain essentially unchanged. The charges on the Ag atoms change the most. The Bader positive charges decrease by ≈0.12−0.13 e difference on each of the Ag atoms, whereas the Hirshfeld charges become 0.07−0.08 e less positive on excitation. The decrease in positive charge of silver atoms upon excitation supports the charge transfer leading to shortening of the bond in the ES structure due to population of the Ag−Ag σ-bonding orbitals.

3.4. Lattice Effect on Light-Induced Distortions. The strong influence of the lattice on the distortion becomes evident when the surrounding lattice is included as is the case in the QM/MM approach (Figure 4). As is clear from Table 1, the observed distortions require the QM/MM theoretical treatment to achieve a reasonably faithful agreement with the observed values. The agreement between theory and experi-

dx.doi.org/10.1021/ic501696y | Inorg. Chem. 2014, 53, 10594−10601

ment of the distance changes is, with one exception, within three times the experimental standard deviations. The exception occurs for the Ag2···Cu1 distance, which contracts by 0.29(3) Å according to the experiment, compared with 0.438 Å according to the QM/MM calculation. This discrepancy between the QM/MM and experimental results may be due to the assumed rigidity of the molecular surrounding and the details of the DFT method and force field employed.

The dominant effect of the surrounding lattice is evident from the geometry as calculated for the isolated molecule (Table 1). As may be expected, in both the singlet and triplet states of the isolated molecule the two copper and silver centers are located symmetrically, leading to either a perfect Z- or parallelogram-type shape, the latter very close to rhombic. In the experimental GS and ES, the molecules are distorted from their ideal symmetry. The Cu2 atom shifts by over 0.30 Å on excitation, whereas Cu1 moves by not more than 0.10 Å (Table 1). This difference is reproduced by the QM/MM optimizations and attributed to differences in the intermolecular interactions. Analysis of the effect of the intermolecular interactions on both the equilibrium and the excited-state structures is clearly of interest but is beyond the scope of the current study.

4. SUMMARY AND CONCLUSIONS

The time-resolved synchrotron pump−probe study of the heteronuclear coinage metal complex with an Ag_2Cu_2 core shows a very large contraction of the core on photoinduced excitation, with the core changing from a Z-shaped pattern to a close-to-rhombic arrangement and the argentophilic interaction contracting from 3.0345(2) to 2.66(3) Å. Theoretical calculations confirm that the contraction is due to LMCT from the methylindole ligands to $\sigma(sp_z)$ orbitals on the silver atoms. The structural change is much better reproduced by the QM/MM calculations than by the theoretical treatment of the isolated complex, indicating the pronounced effect of the solid-state environment on photochemical properties, which cannot be ignored in the design of solid-state-based devices. Because coinage metal complexes show a very large structural variety and interesting unconventional photophysical properties, further studies of the type described here are called for.

■ ASSOCIATED CONTENT

Supporting Information

Details on solid-state spectroscopy, crystallographic data collection and refinement, TR data collection, data processing and refinement procedure, computational methods and results, and a CIF file. This material is available free of charge via the Internet at http://pubs.acs.org.

■ AUTHOR INFORMATION

Corresponding Authors

*(K.N.J.) E-mail: katarzyna.jarzembska@gmail.com.
*(P.C.) E-mail: coppens@buffalo.edu.

Notes

The authors declare no competing financial interest.

■ ACKNOWLEDGMENTS

This research was funded by the National Science Foundation (CHE1213223). The BioCARS Sector 14 is supported by the National Institutes of Health, National Center for Research Resources (RR007707). The APS is sponsored by the U.S. Department of Energy, Office of Basic Energy Sciences (W-31-109-ENG-38). K.N.J. gratefully acknowledges the Polish Ministry of Science and Higher Education for financial support through the "Mobility Plus" program. Assistance from the University at Buffalo Center for Computational Research (CCR) and the Wroclaw Centre for Networking and Superconducting for providing computational facilities for part of this work (grant no. 285) are gratefully acknowledged.

■ REFERENCES

(1) Long, N. J.; Williams, C. K. *Angew. Chem., Int. Ed.* **2003**, *42*, 2586.
(2) Ara, I.; Berenguer, J. R.; Eguizábal, E.; Forniés, J.; Gómez, J.; Lalinde, E. *J. Organomet. Chem.* **2003**, *670*, 221.
(3) Burini, A.; Bravi, R.; Fackler, J. P.; Galassi, R.; Grant, T. A.; Omary, M. A.; Pietroni, B. R.; Staples, R. J. *Inorg. Chem.* **2000**, *39*, 3158.
(4) Crespo, O.; Gimeno, M. C.; Laguna, A.; Lehtonen, O.; Ospino, I.; Pyykkö, P.; Villacampa, M. D. *Chem.—Eur. J.* **2014**, *20*, 3120.
(5) Ford, P. C.; Vogler, A. *Acc. Chem. Res.* **1993**, *26*, 220.
(6) Hissler, M.; McGarrah, J. E.; Connick, W. B.; Geiger, D. K.; Cummings, S. D.; Eisenberg, R. *Coord. Chem. Rev.* **2000**, *208*, 115.
(7) Osawa, M.; Kawata, I.; Ishii, R.; Igawa, S.; Hashimoto, M.; Hoshino, M. *J. Mater. Chem. C* **2013**, *1*, 4375.
(8) Abdou, H. E.; Mohamed, A. A.; López-de-Luzuriaga, J. M.; Monge, M.; Fackler, J. P. *Inorg. Chem.* **2012**, *51*, 2010.
(9) Laguna, A.; Lasanta, T.; López-de-Luzuriaga, J. M.; Monge, M.; Naumov, P.; Olmos, M. E. *J. Am. Chem. Soc.* **2010**, *132*, 456.
(10) Koshevoy, I. O.; Koskinen, L.; Smirnova, E. S.; Haukka, M.; Pakkanen, T. A.; Melnikov, A. S.; Tunik, S. P. *Z. Anorg. Allg. Chem.* **2010**, *636*, 795.
(11) Calhorda, M. J.; Ceamanos, C.; Crespo, O.; Gimeno, M. C.; Laguna, A.; Larraz, C.; Vaz, P. D.; Villacampa, M. D. *Inorg. Chem.* **2010**, *49*, 8255.
(12) Wang, Q.-M.; Lee, Y.-A.; Crespo, O.; Deaton, J.; Tang, C.; Gysling, H. J.; Gimeno, M. C.; Larraz, C.; Villacampa, M. D.; Laguna, A.; Eisenberg, R. *J. Am. Chem. Soc.* **2004**, *126*, 9488.
(13) Fu, W.-F.; Chan, K.-C.; Cheung, K.-K.; Che, C.-M. *Chem.—Eur. J.* **2001**, *7*, 4656.
(14) Irwin, M. J.; Vittal, J. J.; Puddephatt, R. J. *Organometallics* **1997**, *16*, 3541.
(15) Schmidbaur, H. *Chem. Soc. Rev.* **1995**, *24*, 391.
(16) Pyykkö, P. *Chem. Soc. Rev.* **2008**, *37*, 1967.
(17) Mendizabal, F.; Pyykkö, P. *Phys. Chem. Chem. Phys.* **2004**, *6*, 900.
(18) Pyykkö, P. *Angew. Chem., Int. Ed.* **2004**, *43*, 4412.
(19) Catalano, V. J.; Malwitz, M. A. *Inorg. Chem.* **2003**, *42*, 5483.
(20) Paliwoda, D.; Wawrzyniak, P.; Katrusiak, A. *J. Phys. Chem. Lett.* **2014**, *5*, 2182.
(21) Hu, X.-H.; Liang, Y.; Li, C.; Yi, X.-Y. *Dalton Trans.* **2014**, *43*, 2458.
(22) Ai, P.; Danopoulos, A. A.; Braunstein, P.; Monakhov, K. Y. *Chem. Commun.* **2014**, *50*, 103.
(23) Pašteka, L. s. F.; Rajskỳ, T. s.; Urban, M. *J. Phys. Chem. A* **2013**, *117*, 4472.
(24) Koskinen, L.; Jäskeläinen, S.; Oresmaa, L.; Haukka, M. *CrystEngComm* **2012**, *14*, 3509.
(25) Chiarella, G. M.; Melgarejo, D. Y.; Rozanski, A.; Hempte, P.; Perez, L. M.; Reber, C.; Fackler, J. P. *Chem. Commun.* **2010**, *46*, 136.
(26) Tiekink, E. R. T.; Kang, J.-G. *Coord. Chem. Rev.* **2009**, *253*, 1627.
(27) Koshevoy, I. O.; Koskinen, L.; Haukka, M.; Tunik, S. P.; Serdobintsev, P. Y.; Melnikov, A. S.; Pakkanen, T. A. *Angew. Chem., Int. Ed.* **2008**, *47*, 3942.
(28) Pattacini, R.; Barbieri, L.; Stercoli, A.; Cauzzi, D.; Graiff, C.; Lanfranchi, M.; Tiripicchio, A.; Elviri, L. *J. Am. Chem. Soc.* **2006**, *128*, 866.
(29) Wei, Q.-H.; Yin, G.-Q.; Zhang, L.-Y.; Shi, L.-X.; Mao, Z.-W.; Chen, Z.-N. *Inorg. Chem.* **2004**, *43*, 3484.

(30) Fernández, E. J.; López-de-Luzuriaga, J. M.; Monge, M.; Olmos, M. E.; Pérez, J.; Laguna, A.; Mohamed, A. A.; Fackler, J. P. *J. Am. Chem. Soc.* **2003**, *125*, 2022.
(31) Yam, V. W.-W. *Acc. Chem. Res.* **2002**, *35*, 555.
(32) Rawashdeh-Omary, M. A.; Omary, M. A.; Fackler, J. P. *Inorg. Chim. Acta* **2002**, *334*, 376.
(33) Rais, D.; Yau, J.; Mingos, D. M. P.; Vilar, R.; White, A. J. P.; Williams, D. J. *Angew. Chem., Int. Ed.* **2001**, *40*, 3464.
(34) Yam, V. W.-W.; Lo, K. K.-W. *Chem. Soc. Rev.* **1999**, *28*, 323.
(35) Pyykkö, P.; Tamm, T. *Organometallics* **1998**, *17*, 4842.
(36) Omary, M. A.; Webb, T. R.; Assefa, Z.; Shankle, G. E.; Patterson, H. H. *Inorg. Chem.* **1998**, *37*, 1380.
(37) Yam, V. W.-W. *J. Photochem. Photobiol., A* **1997**, *106*, 75.
(38) Yam, V. W.-W.; Yeung, P. K.-Y.; Cheung, K.-K. *Angew. Chem., Int. Ed.* **1996**, *35*, 739.
(39) Forward, J. M.; Bohmann, D.; Fackler, J. P.; Staples, R. J. *Inorg. Chem.* **1995**, *34*, 6330.
(40) King, C.; Wang, J.-C.; Khan, M. N. I.; Fackler, J. P. *Inorg. Chem.* **1989**, *28*, 2145.
(41) Schubert, H.; Wesemann, L. *Organometallics* **2010**, *29*, 4906.
(42) Barreiro, E.; Casas, J. S.; Couce, M. D.; Laguna, A.; López-de-Luzuriaga, J. M.; Monge, M.; Sánchez, A.; Sordo, J.; López, E. M. V. *Dalton Trans.* **2013**, *42*, 5916.
(43) Findeis, B.; Gade, L. H.; Scowen, I. J.; McPartlin, M. *Inorg. Chem.* **1997**, *36*, 960.
(44) Gorol, M.; Mösch-Zanetti, N. C.; Roesky, H. W.; Noltemeyer, M.; Schmidt, H.-G. *Chem. Commun.* **2003**, 46.
(45) Koshevoy, I. O.; Karttunen, A. J.; Lin, Y.-C.; Lin, C.-C.; Chou, P.-T.; Tunik, S. P.; Haukka, M.; Pakkanen, T. A. *Dalton Trans.* **2010**, *39*, 2395.
(46) Fackler, J. P.; Lopez, C. A.; Staples, R. J.; Wang, S.; Winpenny, R. E. P.; Lattimer, R. P. *J. Chem. Soc., Chem. Commun.* **1992**, 146.
(47) Koshevoy, I. O.; Shakirova, J. R.; Melnikov, A. S.; Haukka, M.; Tunik, S. P.; Pakkanena, T. A. *Dalton Trans.* **2011**, *40*, 7927.
(48) Lang, H.; Köhler, K.; Blau, S. *Coord. Chem. Rev.* **1995**, *143*, 113.
(49) Vicente, J.; González-Herrero, P.; García-Sánchez, Y.; Bautista, D. *Inorg. Chem.* **2008**, *47*, 10662.
(50) Sato, T.; Nozawa, S.; Tomita, A.; Hoshino, M.; Koshihara, S.-y.; Fujii, H.; Adachi, S.-i. *J. Phys. Chem. C* **2012**, *116*, 14232.
(51) Lima, F. A.; Milne, C. J.; Amarasinghe, D. C. V.; Rittmann-Frank, M. H.; Veen, R. M. v. d.; Reinhard, M.; Pham, V.-T.; Karlsson, S.; Johnson, S. L.; Grolimund, D.; Borca, C.; Huthwelker, T.; Janousch, M.; Mourik, F. v.; Abela, R.; Chergui, M. *Rev. Sci. Instrum.* **2011**, *82*, 063111.
(52) Bressler, C.; Milne, C.; Pham, V.-T.; ElNahhas; van der Veen, R. M.; Gawelda, W.; Johnson, S.; Beaud, P.; Grolimund, D.; Kaiser, M.; Borca, C. N.; Ingold, G.; Abela, R.; Chergui, M. *Science* **2009**, *323*, 489.
(53) Saes, M.; Bressler, C.; Abela, R.; Grolimund, D.; Johnson, S. L.; Heimann, P. A.; Chergui, M. *Phys. Rev. Lett.* **2003**, *90*, 047403.
(54) Chen, L. X.; Zhang, X. *J. Phys. Chem. Lett.* **2013**, *4*, 4000.
(55) Della-Longa, S.; Chen, L. X.; Frank, P.; Hayakawa, K.; Hatada, K.; Benfatto, M. *Inorg. Chem.* **2009**, *48*, 3934.
(56) Coppens, P. *J. Phys. Chem. Lett.* **2011**, *2*, 616.
(57) Makal, A.; Trzop, E.; Sokolow, J.; Kalinowski, J.; Benedict, J.; Coppens, P. *Acta Crystallogr.* **2011**, *A67*, 319.
(58) Ren, Z.; Bourgeois, D.; Helliwell, J. R.; Moffat, K.; Šrajer, V.; Stoddard, B. L. *J. Synchrotron Rad.* **1999**, *6*, 891.
(59) Schotte, F.; Cho, H. S.; Kaila, V. R. I.; Kamikubo, H.; Dashdorj, N.; Henry, E. R.; Graber, T. J.; Henning, R.; Wulff, M.; Hummer, G.; Kataoka, M.; Anfinru, P. A. *Proc. Natl. Acad. Sci. U.S.A.* **2012**, *109*, 19256.
(60) Kamiński, R.; Graber, T.; Benedict, J. B.; Henning, R.; Chen, Y.-S.; Scheins, S.; Messerschmidt, M.; Coppens, P. *J. Synchrotron Rad.* **2010**, *17*, 479.
(61) Coppens, P.; Pitak, M.; Gembicky, M.; Messerschmidt, M.; Scheins, S.; Benedict, J. B.; Adachi, S.-I.; Sato, T.; Nozawa, S.; Ichiyanagi, K.; Chollet, M.; Koshihara, S.-Y. *J. Synchrotron Rad.* **2009**, *16*, 226.
(62) Kalinowski, J.; Fournier, B.; Makal, A.; Coppens, P. *J. Synchrotron Rad.* **2012**, *19*, 637.
(63) Kalinowski, J.; Makal, A.; Coppens, P. *J. Appl. Crystallogr.* **2011**, *44*, 1182.
(64) Fournier, B.; Coppens, P. *Acta Crystallogr.* **2014**, *A70*, 514.
(65) Makal, A.; Benedict, J.; Trzop, E.; Sokolow, J.; Fournier, B.; Chen, Y.; Kalinowski, J. A.; Graber, T.; Henning, R.; Coppens, P. *J. Phys. Chem. A* **2012**, *116*, 3359.
(66) Benedict, J. B.; Makal, A.; Sokolow, J. D.; Trzop, E.; Scheins, S.; Henning, R.; Graber, T.; Coppens, P. *Chem. Commun.* **2011**, *47*, 1704.
(67) Collet, E.; Moisan, N.; Baldé, C.; Bertoni, R.; Trzop, E.; Laulhé, C.; Lorenc, M.; Servol, M.; Cailleau, H.; Tissot, A.; Boillot, M.-L.; Graber, T.; Henning, R.; Coppens, P.; Cointea, M. B.-L. *Phys. Chem. Chem. Phys.* **2012**, *14*, 6192.
(68) Cailleau, H.; Lorenc, M.; Guérin, L.; Servol, M.; Collet, E.; Cointe, M. B.-L. *Acta Crystallogr.* **2010**, *A66*, 189.
(69) Unit cell parameters of **1**: a = 12.6106(2) Å, b = 14.1988(3) Å, c = 22.0662(4) Å, α = 76.3912(3)°, β = 81.5811(3)°, γ = 66.8814(3)°, V = 3525.30(11) Å^3.
(70) Vorontsov, I.; Pillet, S.; Kamiński, R.; Schmøkel, M. S.; Coppens, P. *J. Appl. Crystallogr.* **2010**, *43*, 1129.
(71) Vorontsov, I. I.; Coppens, P. *J. Synchrotron Rad.* **2005**, *12*, 488.
(72) Szabo, A.; Ostlund, N. S. *Modern Quantum Chemistry*; Dover Publishing: Mineola, NY, 1996.
(73) Parr, R. G.; Yang, W. *Density-Functional Theory of Atoms and Molecules*; Oxford University Press: New York, 1989.
(74) Allen, F. H. *Acta Crystallogr.* **2002**, *B58*, 380.
(75) Allen, F. H.; Bruno, I. J. *Acta Crystallogr.* **2010**, *B66*, 380.
(76) Kamiński, R.; Schmøkel, M. S.; Coppens, P. *J. Phys. Chem. Lett.* **2010**, *1*, 2349.
(77) Kochman, M. A.; Morrison, C. A. *J. Chem. Theory Comput.* **2013**, *9*, 1182.
(78) Kamiński, R.; Jarzembska, K. N.; Domagała, S. *J. Appl. Crystallogr.* **2013**, *46*, 540.
(79) Jean-Ruel, H.; Cooney, R. R.; Gao, M.; Lu, C.; Kochman, M. A.; Morrison, C. A.; Miller, R. J. D. *J. Phys. Chem. A* **2011**, *115*, 13158.
(80) Adamo, C.; Barone, V. *J. Chem. Phys.* **1999**, *110*, 6158.
(81) Perdew, J. P.; Burke, K.; Ernzerhof, M. *Phys. Rev. Lett.* **1996**, *77*, 3865.
(82) Hay, P. J.; Wadt, W. R. *J. Chem. Phys.* **1985**, *82*, 270.
(83) Hay, P. J.; Wadt, W. R. *J. Chem. Phys.* **1985**, *82*, 299.
(84) Dunning, T. H., Jr.; Hay, P. J. *Modern Theoretical Chemistry*; Plenum, New York, 1977; Vol. *3*.
(85) Wadt, W. R.; Hay, P. J. *J. Chem. Phys.* **1985**, *82*, 284.
(86) Frisch, M. J.; Trucks, G. W.; Schlegel, H. B.; Scuseria, G. E.; Robb, M. A.; Cheeseman, J. R.; Scalmani, G.; Barone, V.; Mennucci, B.; Petersson, G. A.; Nakatsuji, H.; Caricato, M.; Li, X.; Hratchian, H. P.; Izmaylov, A. F.; Bloino, J.; Zheng, G.; Sonnenberg, J. L.; Hada, M.; Ehara, M.; Toyota, K.; Fukuda, R.; Hasegawa, J.; Ishida, M.; Nakajima, T.; Honda, Y.; Kitao, O.; Nakai, H.; Vreven, T.; Montgomery, J. A., Jr.; Peralta, J. E.; Ogliaro, F.; Bearpark, M.; Heyd, J. J.; Brothers, E.; Kudin, K. N.; Staroverov, V. N.; Kobayashi, R.; Normand, J.; Raghavachari, K.; Rendell, A.; Burant, J. C.; Iyengar, S. S.; Tomasi, J.; Cossi, M.; Rega, N.; Millam, J. M.; Klene, M.; Knox, J. E.; Cross, J. B.; Bakken, V.; Adamo, C.; Jaramillo, J.; Gomperts, R.; Stratmann, R. E.; Yazyev, O.; Austin, A. J.; Cammi, R.; Pomelli, C.; Ochterski, J. W.; Martin, R. L.; Morokuma, K.; Zakrzewski, V. G.; Voth, G. A.; Salvador, P.; Dannenberg, J. J.; Dapprich, S.; Daniels, A. D.; Farkas, O.; Foresman, J. B.; Ortiz, J. V.; Cioslowski, J.; Fox, D. J. *Gaussian 09*; Gaussian, Inc.: Wallingford, CT, 2009.
(87) Hirshfeld, F. L. *Theor. Chim. Acta* **1977**, *44*, 129.
(88) Bader, R. F. W. *Atoms in Molecules: A Quantum Theory*; Oxford University Press: New York, 1994.
(89) Baerends, E. J.; Ziegler, T.; Autschbach, J.; Bashford, D.; Bérces, A.; Bickelhaupt, F. M.; Bo, C.; Boerrigter, P. M.; Cavallo, L.; Chong, D. P.; Deng, L.; Dickson, R. M.; Ellis, D. E.; Faassen, M. v.; Fan, L.; Fischer, T. H.; Guerra, C. F.; Ghysels, A.; Giammona, A.; Gisbergen, S. J. A. v.; Götz, A. W.; Groeneveld, J. A.; Gritsenko, O. V.; Grüning, M.; Gusarov, S.; Harris, F. E.; Hoek, P. v. d.; Jacob, C. R.; Jacobse, H.;

Jensen, L.; Kaminski, J. W.; Kessel, G. v.; Kootstra, F.; Kovalenko, A.; Krykunov, M. V.; Lenthe, E. v.; McCormack, D. A.; Michalak, A.; Mitoraj, M.; Neugebauer, J.; Nicu, V. P.; Noodleman, L.; Osinga, V. P.; Patchkovskii, S.; Philipsen, P. H. T.; Post, D.; Pye, C. C.; Ravenek, W.; Rodríguez, J. I.; Ros, P.; Schipper, P. R. T.; Schreckenbach, G.; Seldenthuis, J. S.; Seth, M.; Snijders, J. G.; Solà, M.; Swart, M.; Swerhone, D.; Velde, G. t.; Vernooijs, P.; Versluis, L.; Visscher, L.; Visser, O.; Wang, F.; Wesolowski, T. A.; Wezenbeek, E. M. v.; Wiesenekker, G.; Wolff, S. K.; Woo, T. K.; Yakovlev, A. L. *ADF Molecular Modeling Suite*; Scientific Computing & Modelling: Amsterdam, The Netherlands, 2012.

(90) Velde, G. t.; Bickelhaupt, F. M.; Gisbergen, S. J. A. v.; Guerra, C. F.; Baerends, E. J.; Snijders, J. G.; Ziegler, T. *J. Comput. Chem.* **2001**, *22*, 931.

(91) Rodríguez, J. I.; Köster, A. M.; Ayers, P. W.; Santos-Valle, A.; Vela, A.; Merino, G. *J. Comput. Chem.* **2009**, *30*, 1082.

(92) Rodriguez, J. I. *J. Comput. Chem.* **2013**, *34*, 681.

(93) Rodríguez, J. I.; Bader, R. F. W.; Ayers, P. W.; Michel, C.; Goetz, A.; Bo, C. *Chem. Phys. Lett.* **2009**, *472*, 149.

(94) Chong, D. P. *Mol. Phys.* **2005**, *103*, 749.

(95) Chong, D. P.; Lenthe, E. v.; Gisbergen, S. J. A. v.; Baerends, E. J. *J. Comput. Chem.* **2004**, *25*, 1030.

(96) Lenthe, E. v.; Baerends, E. J. *J. Comput. Chem.* **2003**, *24*, 1142.

(97) Perdew, J. P. *Phys. Rev. B* **1986**, *33*, 8822.

(98) Becke, A. D. *Phys. Rev. A* **1988**, *38*, 3098.

(99) Lenthe, E.; Baerends, E. J.; Snijders, J. G. *J. Chem. Phys.* **1993**, *99*, 4597.

(100) Lenthe, E. v.; Baerends, E. J.; Snijders, J. G. *J. Chem. Phys.* **1994**, *101*, 9783.

(101) Lenthe, E. v.; Ehlers, A.; Baerends, E.-J. *J. Chem. Phys.* **1999**, *110*, 8943.

(102) Lenthe, E. v.; Leeuwen, R. v.; Baerends, E. J.; Snijders, J. G. *Int. J. Quantum Chem.* **1996**, *57*, 281.

(103) Lenthe, E. v.; Snijders, J. G.; Baerends, E. J. *J. Chem. Phys.* **1996**, *105*, 6505.

(104) Fournier, B.; Coppens, P. *Acta Crystallogr.* **2014**, *A70*, 291.

(105) Zheng, S.-L.; Messerschmidt, M.; Coppens, P. *Acta Crystallogr.* **2007**, *B63*, 644.

(106) Kim, C. D.; Pillet, S.; Wu, G.; Fullagar, W. K.; Coppens, P. *Acta Crystallogr.* **2002**, *A58*, 133.

(107) Schmøkel, M. S.; Kamiński, R.; Benedict, J. B.; Coppens, P. *Acta Crystallogr.* **2010**, *A66*, 632.

(108) Bondi, A. *J. Phys. Chem.* **1964**, *68*, 441.

(109) Zheng, S.-L.; Volkov, A.; Nygren, C. L.; Coppens, P. *Chem.—Eur. J.* **2007**, *13*, 8583.

(110) Kamiński, R.; Herbaczyńska, B.; Srebro, M.; Pietrzykowski, A.; Michalak, A.; Jerzykiewicz, L. B.; Woźniak, K. *Phys. Chem. Chem. Phys.* **2011**, *13*, 10280.

(111) Farrugia, L. J.; Evans, C.; Senn, H. M.; Hänninen, M. M.; Sillanpää, R. *Organometallics* **2012**, *31*, 2559.

(112) Macchi, P.; Garlaschelli, L.; Sironi, A. *J. Am. Chem. Soc.* **2002**, *124*, 14173.